LETTERS

nature biotechnology

Artificial cell-cell communication in yeast *Saccharomyces cerevisiae* using signaling elements from *Arabidopsis thaliana*

Ming-Tang Chen[1] & Ron Weiss[1,2]

The construction of synthetic cell-cell communication networks can improve our quantitative understanding of naturally occurring signaling pathways and enhance our capabilities to engineer coordinated cellular behavior in cell populations. Towards accomplishing these goals in eukaryotes, we developed and analyzed two artificial cell-cell communication systems in yeast. We integrated *Arabidopsis thaliana* signal synthesis and receptor components with yeast endogenous protein phosphorylation elements and new response promoters. In the first system, engineered yeast 'sender' cells synthesize the plant hormone cytokinin, which diffuses into the environment and activates a hybrid exogenous/endogenous phosphorylation signaling pathway in nearby engineered yeast 'receiver' cells. For the second system, the sender network was integrated into the receivers under positive-feedback regulation, resulting in population density–dependent gene expression (that is, quorum sensing). The combined experimental work and mathematical modeling of the systems presented here can benefit various biotechnology applications for yeast and higher level eukaryotes, including fermentation processes, biomaterial fabrication and tissue engineering.

To demonstrate the feasibility of engineering an artificial communication system between eukaryotic cells, we designed synthetic gene networks that elicited an exchange of information between engineered yeast sender and receiver cells through the synthesis, transmission and reception of plant hormone cytokinin[1]. Yeast senders synthesize cytokinin isopentenyladenine[1] (IP), an adenine derivative involved in growth and development of plants, which diffuses through the cell membrane and into the surrounding environment (**Fig. 1a**). When IP binds the cytokinin receptor AtCRE1 in nearby yeast receivers, AtCRE1 phosphorylates endogenous histidine phospho-transfer protein YPD1 (ref. 2), a protein that regularly shuttles across the nuclear envelope[3]. Phospho-YPD1 phosphorylates the endogenous nuclear aspartate response regulator SKN7 (ref. 3). Phospho-SKN7 subsequently activates the expression of a green fluorescent protein (GFP) from a synthetic promoter P_{SSRE} (synthetic SKN7 response element; **Fig. 1b**).

To ensure that the receiving-signaling pathway works correctly and efficiently, we made several design decisions. The original yeast SLN1-YPD1-SSK1/SKN7 phosphorylation pathway is composed of SLN1 cell-surface osmosensor histidine kinase, YPD1 histidine phospho-transfer protein and a pair of aspartate response regulators, SSK1 and SKN7 (ref. 4). SLN1-YPD1-SSK1 phosphorylation plays an essential role in cell survival in high-osmolarity environments by activation of the HOG1 pathway[5,6]. However, under normal growth conditions HOG1 activity can be lethal. In these conditions, autophosphorylated SLN1 phosphorylates YPD1, resulting in suppression of the HOG1 pathway through SSK1 phosphorylation. But for our engineered receivers, constitutive SLN1 phosphorylation of YPD1 would prevent the detection of cytokinin signaling through AtCRE1 phosphorylation of YPD1, and hence we used a *sln1*Δ strain[5]. The engineered receiver cells also overexpress PTP2, an endogenous HOG1 protein phosphatase[5], which keeps the HOG1 pathway inactive and rescues the *sln1*Δ lethal phenotype.

For our system, SKN7 activation was chosen over SSK1 activation because the latter signal transducer affects many high-osmolarity response genes[6]. In contrast, phospho-SKN7 has been observed to affect only the yeast OCH1 promoter, where SKN7 binds two 13-bp repeat sequences[7]. We fused GFP to the OCH1 promoter, but this construct exhibited an undesirable high level of basal activity (data not shown). To minimize such basal transcriptional activity, two new promoters were constructed from a modified MEL1 promoter[8], one with a single synthetic SKN7 response element (SSRE)[7] and one with a tandem repeat of SSRE (TR-SSRE) (**Fig. 1b**). A yeast-enhanced GFP variant, yEGFP3 (ref. 9), was fused to each of these promoters to create two receiver strains with different responses. **Figure 2a** shows the time-dependent response of the two receivers to exogenous IP (Sigma-Aldrich), whereas **Figure 2b** shows the IP steady-state dosage-response curves. The observed IP dynamic response range of the two receivers (0.1 μM–1 μM) correlates well with previously observed concentrations in plants[10]. Whereas the sensitivity thresholds of the two receivers are similar, the TR-SSRE promoter exhibits an ~sixfold increase in basal GFP expression and a tenfold increase in full activation. Activation of the receiver pathway does not have a significant effect on cell growth, and the integration of this pathway

[1]Departments of Electrical Engineering and [2]Molecular Biology, Princeton University, J319, Engineering Quadrangle, Olden Street, Princeton, New Jersey 08544, USA. Correspondence should be addressed to R.W. (rweiss@princeton.edu).

Received 24 May; accepted 10 October; published online 20 November 2005; doi:10.1038/nbt1162

appeared to have only a minor effect on cell growth when compared with the original *sln1*Δ strain (**Fig. 2c**).

We tested whether expression of AtIPT4 in engineered yeast senders results in the synthesis of IP and communication with receivers. In plants, adenylate isopentenyl-transferases (IPTs) catalyze the isopentenylation of ATP and ADP[11], and subsequently the isopentenylated ATP and ADP (that is, cytokinin nucleotides) are converted to cytokinin-free bases by enzymes involved in purine metabolism[1]. In *Escherichia coli* hosts, expression of recombinant *A. thaliana* IPTs results in IP synthesis[12], whereas recent work has shown that AtIPT4 and *A. thaliana* CYP735A1 can function together in yeast to synthesize transzeatin, a downstream product of IP[13]. In our experiment, SSRE receiver cells were spread homogenously on a Petri dish using a top-agar layer. A paper disk containing senders (expressing AtIPT4 and red fluorescent protein) was placed in the middle of the dish. **Figure 3a** displays four representative time-lapse microscopy fluorescence observations of the senders and receivers along a strip. The curves in **Figure 3b** quantify fluorescence data from seven strips imaged at different time points during this experiment, depicting the spatial gradient of the GFP response and its increase over time. **Figure 3c** shows the fluorescence image of a large portion of the Petri dish after 30 h. In a control experiment with senders lacking AtIPT4, receiver cells did not exhibit any noticeable fluorescence indicating that the GFP gradient is attributed to IP-based cell-cell communication (data not shown).

To demonstrate 'quorum sensing' behavior[14], we integrated the sender and receiver circuits into a single yeast strain (**Fig. 4a**). Two versions of the quorum-sensing network were constructed by placing AtIPT4 under the control of either the SSRE or TR-SSRE promoter. In these configurations, a positive-feedback loop regulates AtIPT4 expression through activation by IP, the product of AtIPT4. GFP expression from an SSRE promoter was used in both variants to quantify network behavior. The yeast quorum sensing functions as follows: (i) when cells are at low population densities, the expression level of AtIPT4 is minimal because the small concentration of extracellular IP does not activate AtCRE1-YPD1-SKN7 phosphorylation, and, as a result, only basal levels of AtIPT4 and IP are present; (ii) upon reaching a sufficiently high cell density, moderately accumulated IP concentrations trigger AtIPT4 transcription; (iii) as cell densities continue to increase, additional expression of AtIPT4 results in considerable IP synthesis and GFP expression. In this artificial system, IP molecules operate in a fashion similar to bacterial quorum-sensing autoinducers[14].

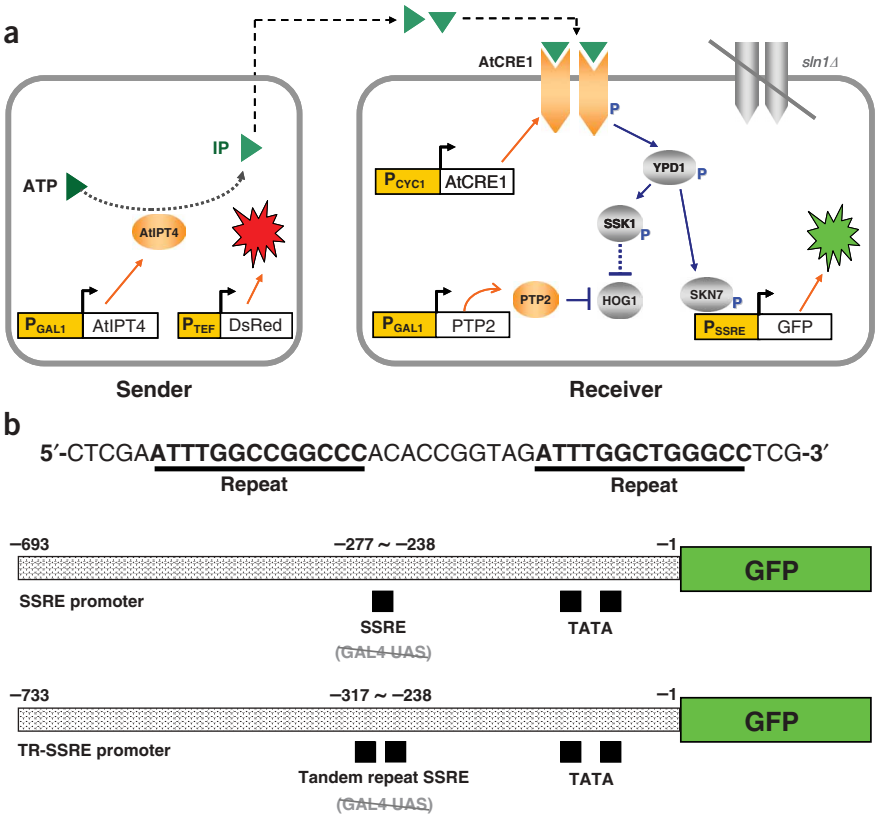

Figure 1 Engineered cytokinin-based sender-receiver communication in yeast. (**a**) Synthetic signaling pathways for sender and receiver cells. All exogenous proteins are shown with their respective promoters (yellow boxes). The sender expresses recombinant *A. thaliana* AtIPT4 under the control of GAL1 promoter. AtIPT4, which catalyzes isopentenylation of ATP, enables the sender to synthesize and secrete IP to nearby receiver cells. The receiver is composed of *A. thaliana* AtCRE1 cytokinin receptor and yeast YPD1 and SKN7 signaling proteins in an *sln1*Δ mutant strain. The receiver cells also overexpress PTP2 in order to suppress *sln1*Δ lethality as a result of the activation of downstream HOG1 kinase by the unphosphorylated SSK1 when cytokinin is absent. When IP signal binds AtCRE1, AtCRE1-YPD1-SKN7 phosphorylation activates GFP expression from the SSRE promoter in receiver cells. (**b**) The DNA sequence of the synthetic SKN7 response element (SSRE) and the structure of two SSRE promoters. The SSRE consists of two 13-bp imperfect repeat (underlined) and synthetic flanking and spacing sequence. In the OCH1 promoter, the wild-type SKN7 response element–spacing sequence contains a Swi4/Swi6 cell-cycle box, whereas SSRE includes a 6-bp *Age*I site-spacing sequence instead to reduce basal transcription activity. The SSRE promoter is a MEL1 promoter derivative in which the wild-type GAL4-binding UAS is replaced by the SSRE sequence (positions –238 to –277 bp). The TR-SSRE promoter contains an 80-bp double SSRE sequence at positions –238 to –317 bp of the same UAS-less MEL1 promoter.

Figure 4b demonstrates yeast quorum-sensing behavior for both strains. In separate experiments, cells with AtIPT4 regulated by either SSRE or TR-SSRE were initially grown to a high population density (OD_{660} of 1.2), then diluted 4,000-fold into fresh medium, and fluorescence intensities and OD_{660} values were recorded over 36 h. The measurements show that initial fluorescence readings were high due to the quorum-sensing behavior. After dilution, GFP fluorescence intensities remained constant for about 6 h, likely reflecting the delay in the dephosphorylation of the signal transduction proteins and initially slower growth rates due to the transition from early stationary phase to log phase. Whereas the phosphorylated half-life of AtCRE1 is unknown, the measured *in vitro* half-lives of phospho-YPD1 and phospho-SKN7 are 4 h[15] and 2.4 h[16], respectively. Once SKN7 was no longer active, transcription of GFP ceased and the fluorescence per average cell decreased owing to cell division and protein degradation at a rate consistent with cell division times of 3 h and reported half-life of yEGFP3 (~7.5 h)[9]. As the population densities reached sufficient levels, quorum-sensing cells quickly began to

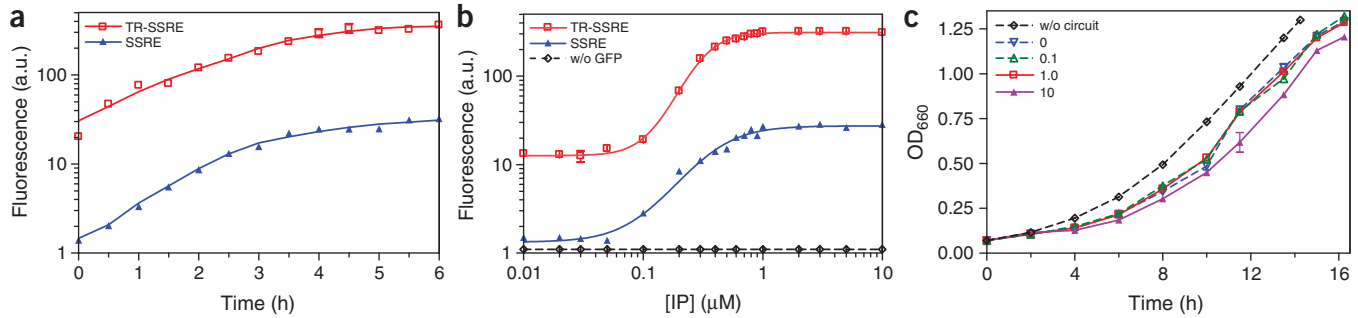

Figure 2 Cytokinin receiver characterization. (**a**) Time-dependent GFP response to cytokinin induction. Exponentially growing (initial OD_{660}, ~0.2) SSRE and TR-SSRE receiver cells were incubated with 10 μM IP and their fluorescence was measured at 30-min time intervals. (**b**) GFP dosage response for SSRE and TR-SSRE receivers incubated with different IP concentrations for 12 h (initial OD_{660}, ~0.1). The GFP negative-control (without GFP) curve represents yeast autofluorescence. (**c**) Growth curves showing OD_{660} as a function of time. The SSRE receiver cells were incubated with different IP concentrations (in μM) for the indicated time and the growth control (without circuit) was *sln1*Δ cells not expressing AtCRE1 and GFP. For **a**, **b** and **c**, symbol markers represent the average measurement values from triplicate experiments, whereas error bars show standard deviation (which are typically <8% and often cannot be observed on the graphs).

fluoresce again due to the accumulation of IP in the medium. The fluorescence of TR-SSRE cells followed the same general pattern as the SSRE cells, but fluorescence began to increase earlier.

To gain a better understanding of the transition between low and high output states, we examined the steady-state behavior of the quorum-sensing systems (**Fig. 4c**). Each quorum-sensing strain was grown in a continuous culture and maintained at various constant densities for 16 h. The steady-state fluorescence intensities showed that the SSRE strain transitions from low to high GFP output between OD_{660} of 0.5 and 0.7, whereas the TR-SSRE transition occurred between OD_{660} of 0.06 and 0.13. Interestingly, both networks exhibited a switch-like response curve. Analysis of a mathematical model (as described in the **Supplementary Note**, **Supplementary Tables 1–4** and **Supplementary Figures 1** and **2** online) suggested that positive-feedback control plays an important role in conferring this all-or-none quorum-sensing response. To validate this hypothesis, we constructed another version of the network where AtIPT4 was constitutively expressed from a GAL1 promoter. As predicted by the model, this system showed a more gradual transition from low to high output as a function of cell density.

For this work, we developed new circuit building blocks for yeast and integrated them with endogenous and exogenous signaling pathways to establish two artificial cell-cell communication systems. We forward engineered these systems from simple and well-characterized components and system behavior was fine tuned by careful choice of network elements. A simple mathematical model was constructed based on published kinetic data and our experimental observations of the receiver and quorum-sensing systems. The model correlated well with experimental observations of all the networks that we constructed, and both the model and the experimental results demonstrated the significance of positive feedback in AtIPT4 regulation. Our work advances the nascent field of synthetic biology[17] by providing and characterizing useful modules for engineering yeast and demonstrating how these modules can be assembled into circuits that coordinate multicellular gene expression. Previous work in synthetic biology has already generated a library of basic and reusable regulatory components and circuits with desired functions in single cells both in bacteria[18] and eukaryotes[19]. In addition, synthetic biology efforts in bacteria have demonstrated basic artificial cell-cell communication[20,21] and more sophisticated synthetic multicellular systems that were built

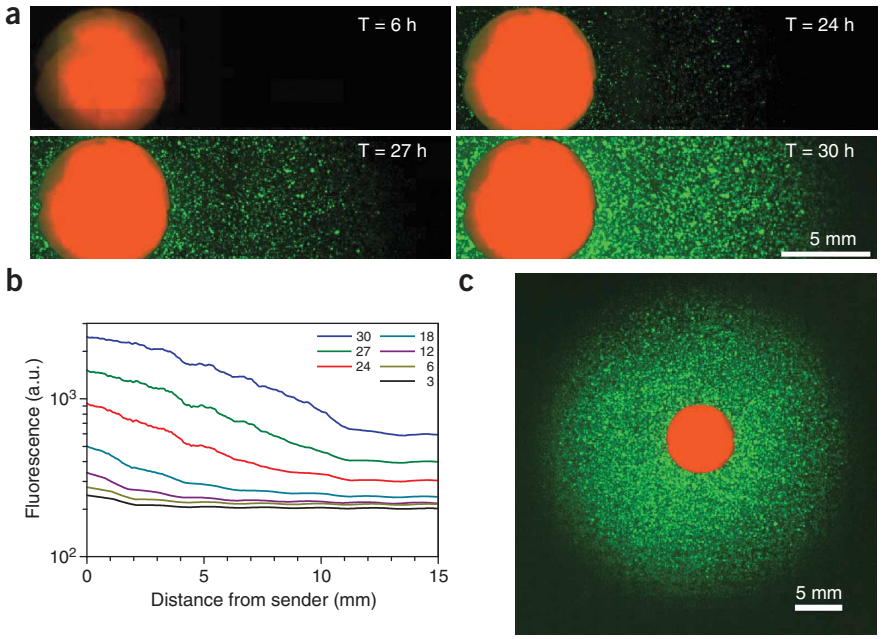

Figure 3 Microscopy observations of sender-receiver communication. (**a**) Fluorescence images of senders and receivers for representative time points. A 13 × 5 grid of green and red fluorescence intensity images were captured with a 2.5× objective and assembled into a single overlay mosaic using custom software. (**b**) Fluorescence intensity curves quantifying average fluorescence at seven different time points (in hours) as a function of distance from the senders. The curves represent a moving average of pixel values within a 0.5 mm × 2 mm rectangular region centered on the vertical axis. (**c**) Fluorescence image of a 26 × 30 grid at the end of 30-h incubation.

using these basic pathways[22–24]. Here we have demonstrated artificial, rationally designed end-to-end intercellular communication and quorum-sensing behavior in eukaryotes.

A few endogenous intercellular signaling pathways have been identified in yeast. For example, the yeast mating pheromone pathway coordinates communication between two cell types and results in cell cycle arrest and transcriptional induction of more than 200 genes[25]. Certain yeast strains are also known to exhibit quorum-sensing-like behavior, such as biofilm formation by the human pathogen *Candida albicans*[26]. However, the signal transduction and regulatory events that regulate these quorum-sensing behaviors are currently not well understood and no direct effects on protein expression have been reported so far. Compared with these endogenous communication pathways, our systems are simple, well-defined, can be easily fine tuned for specific applications, and in principle are useful as modules for the construction of more complex systems. These features facilitate correlation and validation of mathematical models, and can therefore help in the quantitative understanding of other signaling pathways.

The receiver and quorum-sensing circuits presented here can serve as new externally or autonomously inducible gene expression systems that provide spatial and temporal coordination of gene expression among a cell population. These features will benefit a wide variety of biotechnology applications. For example, the programmed coordination of heterologous gene expression in yeast cultures can lower the costs and improve the efficiency of fermentation processes because potentially expensive inducers will no longer be required[27]. It will not be necessary to monitor batch cultures externally, and in the future these might even regulate their own density in a manner similar to the bacterial population control system[28]. Recent advances in engineering yeast metabolism have also enabled expression of a variety of recombinant proteins useful for therapeutic purposes, including humanized glycoproteins[29] and human collagen proteins[30]. The integration of cell-cell communication with such novel target gene expression will enable more complex applications, such as fabrication of spatially complex biomaterials and prototyping of tissue engineering for mammalian cells.

Future development of more complex applications will require the integration of multiple, simultaneously active signaling pathways that have minimal crosstalk with endogenous pathways. For example, engineered receiver circuits based on bacterial quorum-sensing components have been shown in mammalian cells[31–33]. These circuits use hybrid 'R' proteins that respond to acyl-homoserine lactone (AHL) and activate artificial promoters. The implementation of AHL synthases in eukaryotes would expand the set of artificial signaling pathways that can both synthesize and respond to exogenous signals. The engineering of such pathways and integration with more complex intracellular regulation will further advance yeast biotechnological applications.

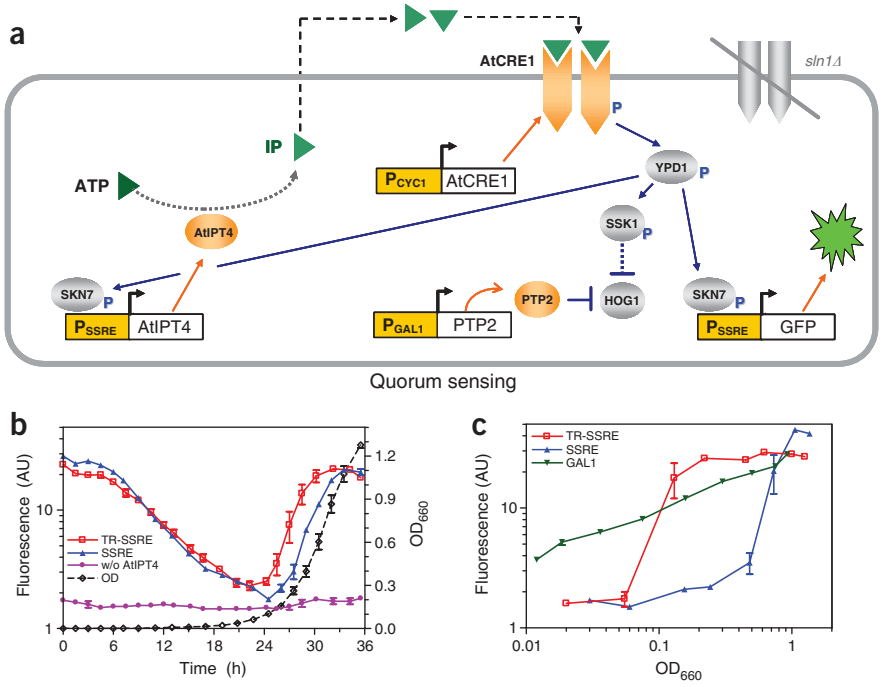

Figure 4 Engineered yeast quorum sensing. (**a**) The sender circuit is integrated into the receiver strain by placing AtIPT4 under the control of an SSRE promoter. (**b**) Characterization of yeast quorum-sensing, time-dependent behavior. Fluorescence intensities and cell densities as a function of time are plotted for cells with SSRE and TR-SSRE regulation of AtIPT4, as well as a negative control (quorum-sensing cells without AtIPT4). The OD_{660} curve represents data from the SSRE experiment. The corresponding OD_{660} curves for TR-SSRE and negative control are essentially identical (data not shown). (**c**) The fluorescence response of continuous cultures for three quorum-sensing networks with AtIPT4 regulated by SSRE, TR-SSRE or GAL1 promoters. Continuous cultures at various constant cell densities were maintained by discrete, periodic dilutions every hour. For **b** and **c** symbol markers represent the average measurement values from triplicate experiments, whereas error bars show standard deviation. AU, arbitrary units.

METHODS

Plasmids. Plasmids and their relevant properties are listed in **Supplementary Table 5** online. Plasmids p413-CYC1[34], p415-CYC1[34] and p416-GAL1[35] were obtained from the American Type Culture Collection. YIpMELα2[8] and pUG27[36] were obtained from EUROSCARF. p415-CYC1-CRE1a[2] and pSVA12[9] were kindly provided by T. Kakimoto and S. Avery, respectively. The SSRE and TR-SSRE promoters were constructed by annealing the SSRE (or TR-SSRE) sequences (**Fig. 1b**) into the *Xho*I site of YIpMELα2. Plasmids p413-SSRE, p413-TR-SSRE and p413-PGAL1 were derived from p413-CYC1 where CYC1 promoter is replaced by the corresponding promoters as indicated by the name of the plasmid. Afterwards, yEGFP3 and yeast ADH1 terminator (T_{ADH1}) coding sequences were digested from pSVA12 and placed under the control of the SSRE and TR-SSRE promoters to construct p413-SSRE-GFP and p413-TR-SSRE-GFP. The created P_{SSRE}-yEGFP3-T_{ADH1} and $P_{TR\text{-}SSRE}$-yEGFP3-T_{ADH1} cassettes were then ligated to the 3′ end of the CYC1 terminator of p415-CYC1-CRE1a (*Eag*I site). These resulted in the receiver plasmids p415-CYC1-CRE1a-SSRE-GFP and p415-CYC1-CRE1a-TR-SSRE-GFP.

AtIPT4 was PCR amplified from *A. thaliana* ecotype *Col* genome. The PCR product was ligated to the GAL1 promoter of p416-GAL1 to create the sender plasmid p416-GAL1-AtIPT4. The quorum-sensing plasmids p413-SSRE-AtIPT4, p413-TR-SSRE-AtIPT4 and p413-PGAL1-AtIPT4 were constructed by fusing AtIPT4 to the p413-SSRE, p413-TR-SSRE and p413-PGAL1 plasmids, respectively. p415-TEF-DsRed-Exp is a p415-CYC1 derivative where DsRed-Exp is expressed by constitutive *Ashbya gossypii* TEF promoter (from pUG27).

Strains and media. *E. coli* strain XL-10 gold (Stratagene) was used for plasmid construction. Yeast strains used in this study are listed in **Supplementary**

Table 6 online. Senders were constructed by transforming yeast YPH500 with p413-CYC1, p415-TEF-DsRed-Exp and p416-GAL1-AtIPT4. Strain TM182α[5] was used for the cytokinin receiver and the quorum-sensing strains. The receiver strains were TM182α carrying p413-SSRE and p415-CYC1-CRE1a-SSRE-GFP (or p415-CYC1-CRE1a-TR-SSRE-GFP). The quorum-sensing strains were TM182α transformed with p415-CYC1-CRE1a-SSRE-GFP and one of p413-SSRE-AtIPT4, p413-TR-SSRE-AtIPT4 or p413-PGAL1-AtIPT4. GFP negative-control strain (**Fig. 2b**) was TM182α with p413-SSRE and p415-CYC1-CRE1a; the growth control strain (**Fig. 2c**) was TM182α with p413-CYC1 and p415-CYC1. The SSRE receiver was used in **Figure 4b** as a quorum-sensing negative-control strain.

Yeast transformation was performed using the LiAc procedure with the standard synthetic dropout (SD) media. For the receiver characterization experiments, IP was obtained from Sigma-Aldrich. For all fluorescence measurements except the GAL1 quorum-sensing strain steady-state experiment, cells were grown in 30 °C in SD Ura$^-$/His$^-$/Leu$^-$ medium with 1% raffinose, 2% galactose and the yeast nitrogen base without riboflavin and folic acid[37]. This medium was used because it has negligible background fluorescence. The GAL1 quorum-sensing strain steady-state experiment was performed in a 2% raffinose and 0.05% galactose medium. The reduced galactose concentration was used to decrease the expression level of AtIPT4 so that GAL1-activation levels more closely resemble SSRE promoter–activation levels.

Flow cytometry & microscopy. For all liquid experiments, GFP intensities were analyzed by fluorescence-activated cell sorting (FACS) using a Beckman Coulter Altra flow cytometer equipped with a 488-nm argon excitation laser and a 515–545 nm emission filter. FACS measurements were calibrated using Spherotech Rainbow Calibration Particles (RCP-30-5A). For each sample, 15,000 events were collected, and their median fluorescence was reported. Line fitting was performed using PRISM analysis software (GraphPad) with either line-smoothing, direct connection or sigmoidal fits.

The sender-receiver solid phase experiment was performed in 30 °C and observations were carried out using a Zeiss Axiovert 200M epifluorescence microscope equipped with a 1344 × 1024 pixel cooled ORCA-ER CCD camera (Hamamatsu Corporation) and a 2.5× objective. A receiver culture was grown to an OD_{660} of 1.0 in liquid media. About 2×10^7 receiver cells were diluted into 2 ml of 0.7% agarose and spread evenly on top of a 2% agarose plate. A sender culture was grown in liquid medium simultaneously to an OD_{660} of 1.0 and concentrated 20-fold. About 1×10^7 cells were spotted on a paper disk 7 mm in diameter and placed in the middle of the dish. Fluorescence images were captured every 3 h. False coloring was performed by capturing images with the appropriate colors and assembling them into larger mosaics using custom software (GFP filters: 470/40 excitation & 525/50 emission, DsRed-Express: 565/30 & 620/60).

Note: Supplementary information is available on the Nature Biotechnology website.

ACKNOWLEDGMENTS

We thank Y. Gerchman, D. Karig, S. Basu and S. Subramanian for helpful discussions. We also thank T. Kakimoto and S. Avery for the gift of yeast strain and plasmids and R. Kerstetter for *A. thaliana* genomic DNA extract. This work was supported by a Burroughs Wellcome Fund fellowship.

COMPETING INTERESTS STATEMENT

The authors declare that they have no competing financial interests.

Published online at http://www.nature.com/naturebiotechnology/
Reprints and permissions information is available online at http://npg.nature.com/reprintsandpermissions/

1. Mok, D.W. & Mok, M.C. Cytokinin metabolism and action. *Annu. Rev. Plant Physiol. Plant Mol. Biol.* **52**, 89–118 (2001).
2. Inoue, T. *et al.* Identification of CRE1 as a cytokinin receptor from *Arabidopsis*. *Nature* **409**, 1060–1063 (2001).
3. Lu, J.M., Deschenes, R.J. & Fassler, J.S. *Saccharomyces cerevisiae* histidine phosphotransferase Ypd1p shuttles between the nucleus and cytoplasm for SLN1-dependent phosphorylation of Ssk1p and Skn7p. *Eukaryot. Cell* **2**, 1304–1314 (2003).
4. Li, S. *et al.* The yeast histidine protein kinase, Sln1p, mediates phosphotransfer to two response regulators, Ssk1p and Skn7p. *EMBO J.* **17**, 6952–6962 (1998).
5. Maeda, T., Wurgler-Murphy, S.M. & Saito, H. A two-component system that regulates an osmosensing MAP kinase cascade in yeast. *Nature* **369**, 242–245 (1994).
6. Hohmann, S. Osmotic stress signaling and osmoadaptation in yeasts. *Microbiol. Mol. Biol. Rev.* **66**, 300–372 (2002).
7. Li, S. *et al.* The eukaryotic two-component histidine kinase Sln1p regulates OCH1 via the transcription factor, Skn7p. *Mol. Biol. Cell* **13**, 412–424 (2002).
8. Melcher, K., Sharma, B., Ding, W.V. & Nolden, M. Zero background yeast reporter plasmids. *Gene* **247**, 53–61 (2000).
9. Mateus, C. & Avery, S.V. Destabilized green fluorescent protein for monitoring dynamic changes in yeast gene expression with flow cytometry. *Yeast* **16**, 1313–1323 (2000).
10. Suzuki, T. *et al.* The *Arabidopsis* sensor His-kinase, AHK4, can respond to cytokinins. *Plant Cell Physiol.* **42**, 107–113 (2001).
11. Kakimoto, T. Biosynthesis of cytokinins. *J. Plant Res.* **116**, 233–239 (2003).
12. Takei, K., Sakakibara, H. & Sugiyama, T. Identification of genes encoding adenylate isopentenyltransferase, a cytokinin biosynthesis enzyme, in *Arabidopsis thaliana*. *J. Biol. Chem.* **276**, 26405–26410 (2001).
13. Takei, K., Yamaya, T. & Sakakibara, H. *Arabidopsis* CYP735A1 and CYP735A2 encode cytokinin hydroxylases that catalyze the biosynthesis of trans-Zeatin. *J. Biol. Chem.* **279**, 41866–41872 (2004).
14. Miller, M.B. & Bassler, B.L. Quorum sensing in bacteria. *Annu. Rev. Microbiol.* **55**, 165–199 (2001).
15. Janiak-Spens, F., Sparling, D.P. & West, A.H. Novel role for an HPt domain in stabilizing the phosphorylated state of a response regulator domain. *J. Bacteriol.* **182**, 6673–6678 (2000).
16. Janiak-Spens, F. & West, A.H. Functional roles of conserved amino acid residues surrounding the phosphorylatable histidine of the yeast phosphorelay protein YPD1. *Mol. Microbiol.* **37**, 136–144 (2000).
17. Ferber, D. Synthetic biology. Microbes made to order. *Science* **303**, 158–161 (2004).
18. Weiss, R. *et al.* Genetic circuit building blocks for cellular computation, communications, and signal processing. *Nat. Comput.* **2**, 47–84 (2003).
19. Kramer, B.P., Fischer, C. & Fussenegger, M. BioLogic gates enable logical transcription control in mammalian cells. *Biotechnol. Bioeng.* **87**, 478–484 (2004).
20. Weiss, R. & Knight, T.F. in *DNA computing, Lecture Notes in Computer Science,* vol. 2054 (eds. Condon, A. & Rozenberg, G.) 1–16, (Springer, New York, 2001).
21. Bulter, T. *et al.* Design of artificial cell-cell communication using gene and metabolic networks. *Proc. Natl. Acad. Sci. USA* **101**, 2299–2304 (2004).
22. Basu, S., Mehreja, R., Thiberge, S., Chen, M.T. & Weiss, R. Spatiotemporal control of gene expression with pulse-generating networks. *Proc. Natl. Acad. Sci. USA* **101**, 6355–6360 (2004).
23. Basu, S., Gerchman, Y., Collins, C.H., Arnold, F.H. & Weiss, R. A synthetic multicellular system for programmed pattern formation. *Nature* **434**, 1130–1134 (2005).
24. Kobayashi, H. *et al.* Programmable cells: interfacing natural and engineered gene networks. *Proc. Natl. Acad. Sci. USA* **101**, 8414–8419 (2004).
25. Bardwell, L. A walk-through of the yeast mating pheromone response pathway. *Peptides* **25**, 1465–1476 (2004).
26. Chen, H., Fujita, M., Feng, Q., Clardy, J. & Fink, G.R. Tyrosol is a quorum-sensing molecule in *Candida albicans*. *Proc. Natl. Acad. Sci. USA* **101**, 5048–5052 (2004).
27. Farmer, W.R. & Liao, J.C. Improving lycopene production in *Escherichia coli* by engineering metabolic control. *Nat. Biotechnol.* **18**, 533–537 (2000).
28. You, L., Cox, R.S., III, Weiss, R. & Arnold, F.H. Programmed population control by cell-cell communication and regulated killing. *Nature* **428**, 868–871 (2004).
29. Wildt, S. & Gerngross, T.U. The humanization of N-glycosylation pathways in yeast. *Nat. Rev. Microbiol.* **3**, 119–128 (2005).
30. Toman, P.D. *et al.* Production of recombinant human type I procollagen trimers using a four-gene expression system in the yeast *Saccharomyces cerevisiae*. *J. Biol. Chem.* **275**, 23303–23309 (2000).
31. Weber, W. *et al.* Engineered *Streptomyces* quorum-sensing components enable inducible siRNA-mediated translation control in mammalian cells and adjustable transcription control in mice. *J. Gene Med.* **7**, 518–525 (2005).
32. Williams, S.C. *et al.* *Pseudomonas aeruginosa* autoinducer enters and functions in mammalian cells. *J. Bacteriol.* **186**, 2281–2287 (2004).
33. Neddermann, P. *et al.* A novel, inducible, eukaryotic gene expression system based on the quorum-sensing transcription factor TraR. *EMBO Rep.* **4**, 159–165 (2003).
34. Mumberg, D., Muller, R. & Funk, M. Yeast vectors for the controlled expression of heterologous proteins in different genetic backgrounds. *Gene* **156**, 119–122 (1995).
35. Mumberg, D., Muller, R. & Funk, M. Regulatable promoters of *Saccharomyces cerevisiae*: comparison of transcriptional activity and their use for heterologous expression. *Nucleic Acids Res.* **22**, 5767–5768 (1994).
36. Gueldener, U., Heinisch, J., Koehler, G.J., Voss, D. & Hegemann, J.H. A second set of loxP marker cassettes for Cre-mediated multiple gene knockouts in budding yeast. *Nucleic Acids Res.* **30**, e23 (2002).
37. Sheff, M.A. & Thorn, K.S. Optimized cassettes for fluorescent protein tagging in *Saccharomyces cerevisiae*. *Yeast* **21**, 661–670 (2004).